

Coordination and Photoisomerization of Azobenzene-Amino Acid Schiff Base Copper(II) Complexes to Lysozyme

Yuto Kuroda, Ryotaro Miyazaki, Daiki Shimonishi, Daisuke Nakane, Takashi Akitsu*

Department of Chemistry, Faculty of Science, Tokyo University of Science, Tokyo, Japan

Email: *akitsu2@rs.tus.ac.jp

How to cite this paper: Kuroda, Y., Miyazaki, R., Shimonishi, D., Nakane, D. and Akitsu, T. (2023) Coordination and Photoisomerization of Azobenzene-Amino Acid Schiff Base Copper(II) Complexes to Lysozyme. *Journal of Materials Science and Chemical Engineering*, 11, 34-44.

<https://doi.org/10.4236/msce.2023.113003>

Received: March 2, 2023

Accepted: March 28, 2023

Published: March 31, 2023

Copyright © 2023 by author(s) and Scientific Research Publishing Inc. This work is licensed under the Creative Commons Attribution International License (CC BY 4.0).

<http://creativecommons.org/licenses/by/4.0/>



Open Access

Abstract

In this study, we exhibited an amino acid (arginine and threonine) derivative Schiff base copper(II) complexes incorporating an azobenzene moiety as a photoresponsive site and conjugated it to egg white lysozyme, a well-known protein, to change ligand conformation under binding to lysozyme. Among several spectroscopic investigations, ESR clearly showed that the nitrogen atom of the amino acid residue of lysozyme was bound to the paramagnetic copper(II) ion of the complex, and UV light irradiation confirmed photoisomerization of the azobenzene moiety of the ligand to cis-form. The binding mode was considered by means of spectroscopic as well as computational methods, whereas complete crystallographic verification was still a preliminary stage.

Keywords

Azobenzene, Schiff Base, Copper, Amino Acid, Lysozyme, Artificial Metalloprotein

1. Introduction

A search of the three-dimensional structures of proteins registered in the Protein Data Bank in 2008 revealed that approximately 40% of the proteins were bound to metal ions [1]. Furthermore, in recent years, by conjugating unnatural metal ions or artificially synthesized metal complexes to proteins, there has been active research into artificial metalloproteins that have new catalytic activities, chemical functions, and reactivity not found in nature [2]. Such artificial metalloproteins may be expected to have a wide range of applications, including cata-

lysts and biomaterials with electronic, magnetic, and medical properties. There are four main strategies for constructing artificial metalloproteins: the strategy of coordinating a metal complex to a protein; the method of substituting a different metal for the metal originally contained in the metalloproteins; strategy to immobilize proteins by supramolecular interactions such as hydrogen bonding; immobilization by covalent bonding of ligand functional groups and protein functional groups strategy [3].

By the way, azobenzene is one of the most utilized photoswitches due to its high quantum yield, stability, and ease of synthesis and derivatization. Since the wavelength of photoisomerization is in the ultraviolet-visible (UV-vis) region (E \rightarrow Z: 380 nm, Z \rightarrow E: > 400 nm), it may be harmful to cells and tissues, and there is a strong concern for medical applications. In parallel with research on the long-wavelength action of isomerization, many studies have also been conducted on conjugating azo compounds to proteins to impart photo-responsiveness [4]. Among previous studies, azo-metal complexes are thought to be able to control the redox potential that may potentially affect SOD and other factors. There is also research that has constructed a molecular synchronization system that controls binding and detachment with copper(II)/copper(I) oxidation-reduction reaction [5], but there are few examples of research that has actually been applied to proteins.

In this study, by incorporating an azobenzene site with high quantum yield and photostability as a photoresponsive site into a Schiff base copper(II) complex containing an amino acid as a ligand, the photo-responsiveness of a protein (egg white lysozyme) was investigated. Therefore, we approach the selection of amino acid ligands that can be expected to combine with lysozyme as molecular design from a computational chemistry approach. We spectroscopically evaluate the combination of lysozyme and copper(II) complexes in solution mainly.

2. Methods

2.1. General Procedures and Physical Measurements

Chemical reagents were purchased from Sigma-Aldrich (St. Louis, MO, USA), WAKO (Osaka, Japan), and TCI (Tokyo, Japan). All the reagents were of the highest commercial grade and were used without further purification.

Infrared (IR) spectra were recorded on a JASCO FT-IR 4200 spectrophotometer in the range of 4000 - 400 cm^{-1} at 298 K. The UV-Vis spectra were measured on a JASCO V-570 spectrophotometer in the range of 800 - 250 nm at 298 K. The circular dichroism (CD) spectra were measured by using a JASCO J-725 at 298 K. The fluorescence spectra were measured on a JASCO FP-6200 spectrophotometer at 298 K. Electron paramagnetic resonance (EPR) spectra of the complexes were recorded on a Bruker EMX-nano EPR spectrometer (X-band) at 77 K. The electrochemical properties of the complexes were measured by cyclic voltammetry (CV) in a 0.1 M of phosphate buffer solution (pH 7.0) with glassy carbon, Pt-wire, and Ag/AgCl electrodes as the working, counter, and reference

electrodes, respectively, using ALS/DY2323 BI-POTENTIOSTAT. The CV curves were measured in three cycles under a nitrogen atmosphere at room temperature with a potential sweep rate of 5 - 200 mVs⁻¹.

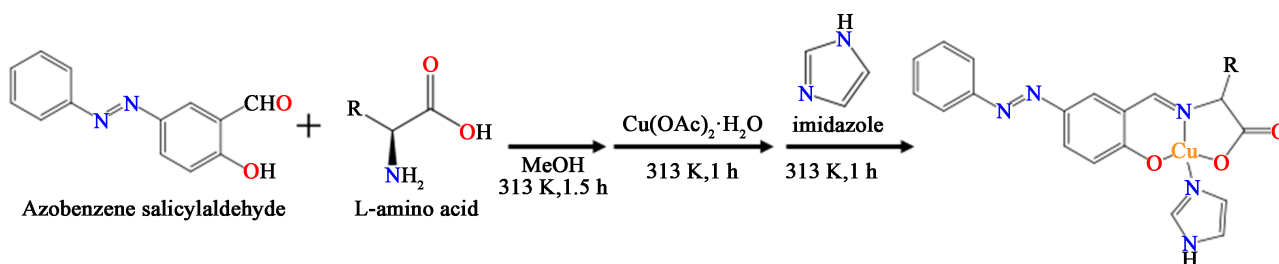
2.2. Preparations of Complexes

CuAT-Imi: Azobenzene-salicylaldehyde [6] (226 mg, 1.00 mmol) and *L*-threonine (119 mg, 1.00 mmol) were dissolved in methanol (100 mL) and stirred at 313 K for 1.5 hr to give a red solution. Copper(II) acetate-hydrate (199 mg, 1.00 mmol) was added and stirred for 1 hr, and imidazole (68 mg, 1.0 mmol) was added and stirred for another hour to give a dark green solution. The reaction solution was allowed to stand at 298 K for 4 days to obtain green needle crystals. Yield: 0.325 g (73.36%). Anal.: C; 48.21% H; 5.15% N; 20.45% Calc. for: C₂₀H₁₉N₅O₄Cu·2H₂O Found.: C; 48.36% H; 4.97% N; 19.85% (**Scheme 1**).

CuAA-Imi: Azobenzene-salicylaldehyde [6] (226 mg, 1.00 mmol) and *L*-arginine (174 mg, 1.00 mmol) were dissolved in methanol (100 mL) and stirred at 313 K for 1.5 hrs to give a red solution. Copper(II) acetate-hydrate (199 mg, 1.00 mmol) was added and stirred for 1 hr, and imidazole (68 mg, 1.0 mmol) was added and stirred for another hour to give a dark green solution. The reaction solution was allowed to stand at 298 for 4 days to obtain green needle crystals. Yield: 0.325 g (73.36%). Anal.: C; 52.06% H; 4.26% N; 15.18% Calc. for: C₂₀H₁₉N₅O₄Cu·0.25H₂O Found.: C; 52.15% H; 4.10% N; 15.18%.

2.3. Computational Methods

Quantum chemistry calculations were performed using Gaussian09 software for 19 types of azobenzene-*L*-amino acid Schiff base copper complex models on GaussView. The calculations performed are structural optimization, vibrational calculations, and excited state calculations. By using B3LYP as the functional, different ones were applied to Cu and CHNO. The accuracy of structural optimization and vibration calculation was improved by increasing CHNO stepwise from 3 - 21 g, 6 - 31 g, and 6 - 31 g (D). In addition, in the calculation of Cu atoms, by specifying the effective core potential (ECP), the calculation amount is reduced by replacing the influence of the core electrons with the potential that the valence electrons feel from the core electrons. LanL2DZ was used for both the basis set for valence electrons and the basis set for ECP.



Scheme 1. Preparation and molecular structures of CuAT-Imi and CuAA-Imi. R denotes substitution groups of the respective amino acids.

Docking simulation to lysozyme was calculated using GOLD software. 5 lyt was selected from the PDB site for the protein lysozyme, and the structure of the ligand complex was optimized by DFT calculation. All water molecules contained in 5 lyt were removed, judging that they were not involved in docking. The scope of ligand docking is the entire lysozyme, and we decide which site is best for docking. GoldScore was selected as the scoring function, and calculations were performed with hydrogen bonds and van der Waals forces as the main elements of the calculation. Based on the GoldScore value, we will determine which complexes are effective for docking to lysozyme. Docking used a genetic algorithm and set the number of trials to 30.

3. Results

The structure of the complex was characterized by FT-IR spectra using the KBr tablet method. Absorption bands corresponding to the imine ν ($-\text{C}=\text{N}$) vibrations of CuAA, CuAT (without imidazole for binding to lysozyme), CuAA-Imi and CuAT-Imi were observed in the range from 1629 to 1635 cm^{-1} . An absorption band corresponding to the ν ($-\text{COO}$) vibration was also observed in the range from 1382 to 1392 cm^{-1} . The assignment was similar to the analogous compounds [6]. Compared with the simulated IR spectra from DFT calculations, ν ($-\text{C}=\text{N}$) vibrations are observed especially in the range of 1656 to 1669 cm^{-1} , which corresponds to the experimental results. This suggests the confirmation of all four complexes as well as preliminary crystal structures from powder X-ray patterns (not shown).

From the two-dimensional fluorescence spectra at an excitation light of 280 nm, the maximum fluorescence wavelength of CuAA increased from 407 nm to 415 nm, and the maximum fluorescence wavelength of CuAT increased from 407 nm to 414 nm with the addition of the copper(II) complex. Long-wavelength shifts were observed. This is due to the deprotonation of the terminal $-\text{OH}$ group to tyrosinate at sites Tyr20 and Tyr23, amino acid residues of lysozyme, or the direct coordination of copper(II) complexes to the $-\text{OH}$ groups of Tyr residues. Therefore, fluorescence intensity quenching suggests binding of lysozyme and copper(II) complexes, CuAA and CuAT. To further understand the fluorescence quenching mechanism, the obtained fluorescence data were analyzed using conventional relationship of Stern-Volmer equation showing a good linear relationship (Figure 1). This indicates a single quenching mechanism (static or dynamic). These results suggested the combination of copper(II) complex and lysozyme.

CD as well as UV-vis spectroscopy for the secondary structural changes of lysozyme in solutions was used to investigate changes in protein secondary structure after binding these complexes. The CD spectrum (not shown) of lysozyme usually shows the strongest negative band at 208 nm and a shoulder peak around 222 nm, characteristic of α -helical, β -sheet structured proteins. In the present study, up to 2 equivalents of CuAA and CuAT were added, but no significant

changes in the spectrum were observed at wavelengths around 208 and 222 nm, which are derived from the secondary structure of lysozyme. From the above, it is suggested that the secondary structure of lysozyme is maintained by the addition of the complexes, and that the lysozyme and the complexes are combined at sites that do not affect the secondary structure of the protein.

The interaction of lysozyme and copper complexes in solution (acetate buffer) was evaluated by UV-vis spectra (Figure 2). The absorption wavelength corresponding to the d-d transition of copper(II) in CuAA shifts from 666 nm to 652 nm as the lysozyme concentration increases, short-wavelength shift similar to CuAA-Imi. This indicates that the copper(II) ion of CuAA is bound to the imidazole group of the histidine (or nitrogen atom containing) residue of lysozyme. Of the residues that make up lysozyme, only one histidine (His15) is on the opposite side of the lysozyme's active site cleft. Therefore, CuAA may be considered bound to His15 on the surface of lysozyme. Additionally, the results of photoisomerization of azobenzene moiety in a composite solution are also shown (Figure 2). Both CuAA and CuAT in mixed solutions with lysozyme showed a decrease in peaks after UV light irradiation (due to cis form of azobenzene) and an increase in peaks after visible light irradiation (due to trans form of azobenzene). Photosomerization was not reversible fully.

Next, we investigated the coordination environment around the central copper metal by means of ESR, and compared the coordination structures and

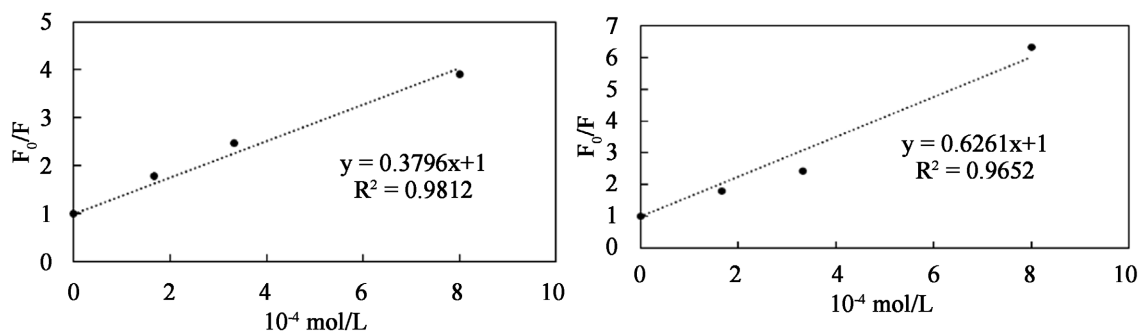


Figure 1. Stern-Volmer equation due to fluorescence quenching of lysozyme ($\lambda_{ex} = 280$ nm, $\lambda_{em} = 415$ nm) by CuAA (left) and CuAT (right).

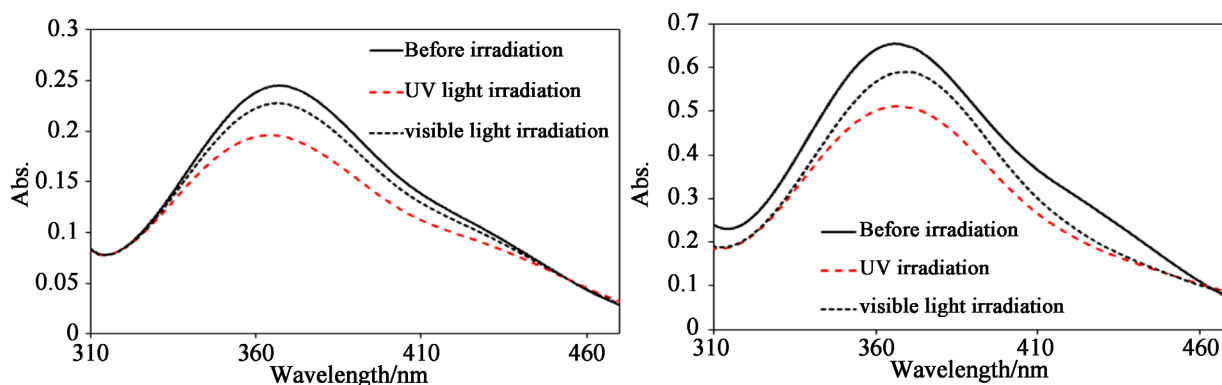


Figure 2. UV-vis spectra of CuAA (left) and CuAT (right) binding lysozyme before and after UV or visible light irradiation.

bonding modes in composite solutions (Figure 3). The ESR spectra of CuAA and CuAA@ Lysozyme were recorded at -196°C , the coordination environment of the paramagnetic ($S = 1/2$) copper(II) site was analyzed. The ESR spectrum of CuAA showed a broad signal with $g_{\text{parallel}} = 2.257$ and $g_{\text{perpendicular}} = 2.056$, whereas CuAA@lysozyme had $g_{\text{parallel}} = 2.268$ and $g_{\text{perpendicular}} = 2.077$, showing a planar or square pyramidal structure around the metal atom. The ESR spectrum of CuAT showed a broad signal with $g_{\text{parallel}} = 2.269$ and $g_{\text{perpendicular}} = 2.062$, while CuAT@ Lysozyme had $g_{\text{parallel}} = 2.272$ and $g_{\text{perpendicular}} = 2.082$. In A_{parallel} , 187.5 G was obtained for CuAA, 176.8 G for CuAA@lysozyme, 183.7 G for CuAT, and 175.2 G for CuAT@ Lysozyme. The observed large values and g_{parallel} smaller than that of the blue copper protein closely resemble the ESR spectrum of the Type-2 copper protein, suggesting that the copper(II) complex is planar. Alternatively, it can be combined with lysozyme while maintaining the square pyramidal structure.

Of course, the CV of lysozyme aqueous solution did not show redox peaks solely. The CV of CuAA (CuAT, CuAA@Lysozyme) showed clear peaks in both oxidation and reduction waves (Figure 4). The CV of CuAT and CuAT@Lysozyme showed different shapes, suggesting that there was almost no copper(II) complex released from lysozyme (Figure 5). The CuAA peak reduction wave (I_a) and oxidation wave (I_b) values correspond to $E = 0.116\text{ V}$, -0.459 V vs. Ag/AgCl (saturated KCl) hereafter abbreviated as KCl), 0.315 V , -0.260 V vs. NHE, and

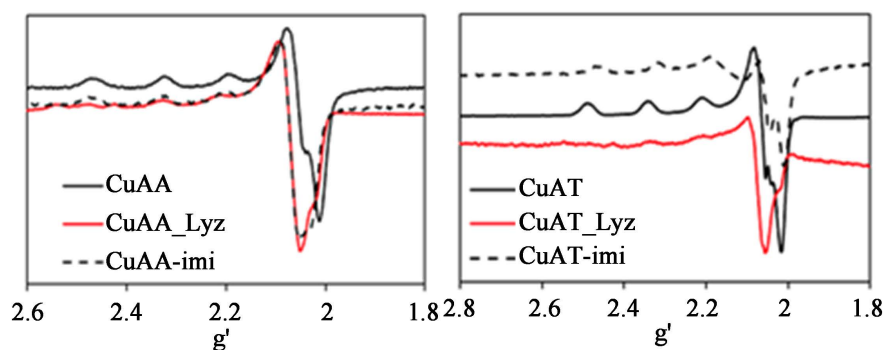


Figure 3. ESR spectra of CuAA (left) and CuAT (right) as binding water or methanol solvents (without mark), lysozyme (Lyz; CuAA@Lysozyme, CuAT@Lysozyme), or imidazole (imi; CuAA-Imi, CuAT-Imi) ligand.

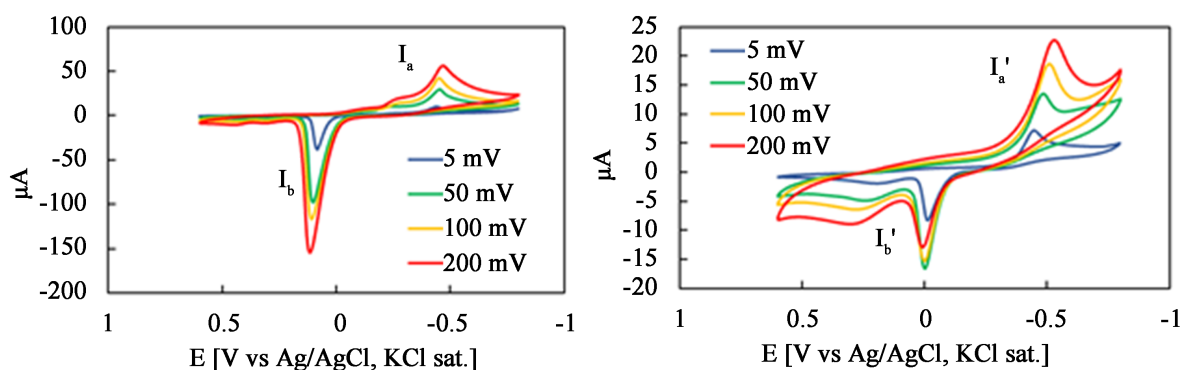


Figure 4. CV of CuAA (right) and CuAA@Lysozyme under different conditions.

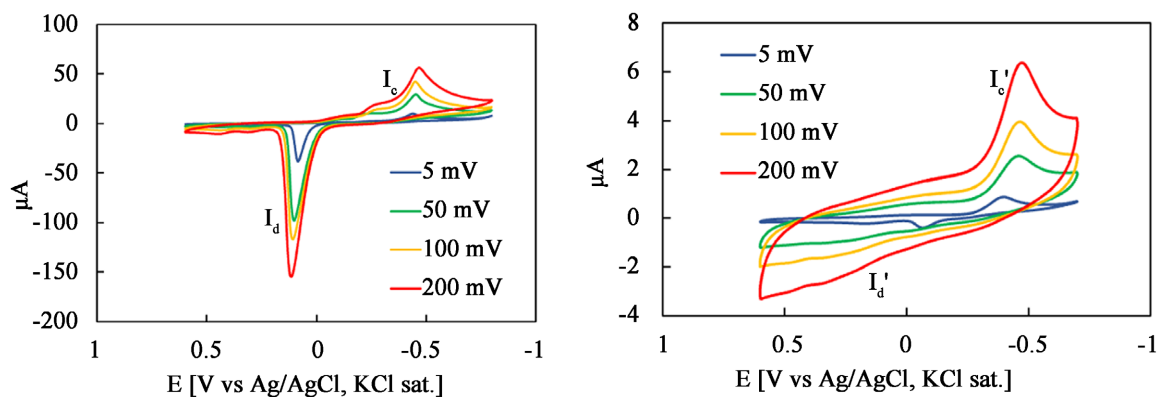


Figure 5. CV of CuAT (right) and CuAT@Lysozyme under different conditions.

CuAA@Lysozyme. The values of the reduction wave (I_a') and the oxidation wave (I_b') of KCl correspond to -0.067 V, -0.447 V vs. Ag/AgCl (KCl), 0.132 V, -0.248 vs. NHE. The values of peak reduction wave I_c and oxidation wave I_d of CuAT correspond to $E = 0.020$ V, -0.365 V vs. Ag/AgCl (KCl), 0.219 V, -0.166 V vs. NHE. The values of wave I_c' and oxidation wave I_d' are -0.012 V, -0.472 V vs. Ag/AgCl (KCl), 0.187 V, -0.271 vs. NHE. Complex CuAT in the presence of lysozyme obscured the oxidation and reduction peaks with increasing sweep rate. From these results, the decrease in the peak current of the CuAT complex after the addition of lysozyme is due to the increase in the viscosity of the solution as a whole with the addition of lysozyme and the binding of the complex CuAT to the bulky and slow lysozyme diffusion coefficient.

4. Discussion

Electrostatic potential maps of 19 azobenzene-amino acid Schiff base copper(II) complexes are depicted (Figure 6). The red area represents the area showing negative values, and the blue area represents the area showing positive values. Focusing on the copper atom, its numerical value is in the range of $+0.70$ to 0.72 , and it is shown that it does not depend on the amino acid ligand used for synthesis. This suggests that the bulkiness of the molecule itself and the electronic properties of the functional groups have an effect on the conjugation of the complexes to lysozyme.

As for promising candidates for docking among them, two complexes were actually selected after computational screening as experimental results presented. CuAA showed the highest Gold score (50.4975) for docking inside the hydrophobic pocket of lysozyme (Figure 7). The docking was completed by the entry of the Arg site rather than the copper site into the hydrophobic pocket. Amino acid residues of lysozyme present in the vicinity include ASN (46)/THR (47)/ASP (52)/ASN (59), respectively 2.034 Å, 2.173 Å, $1.971/2.065$ Å from the complex, respectively. The distance was 1.925 Å. ASN (46)/THR (47) are close to the copper site of the complex, and ASP (52)/ASN (59) are close to the -NH hydrogen of the Arg site via hydrogen bonding. The Arg site has two -NH₂ at the end, and two hydrogen bonds with ASP (52) can be confirmed.

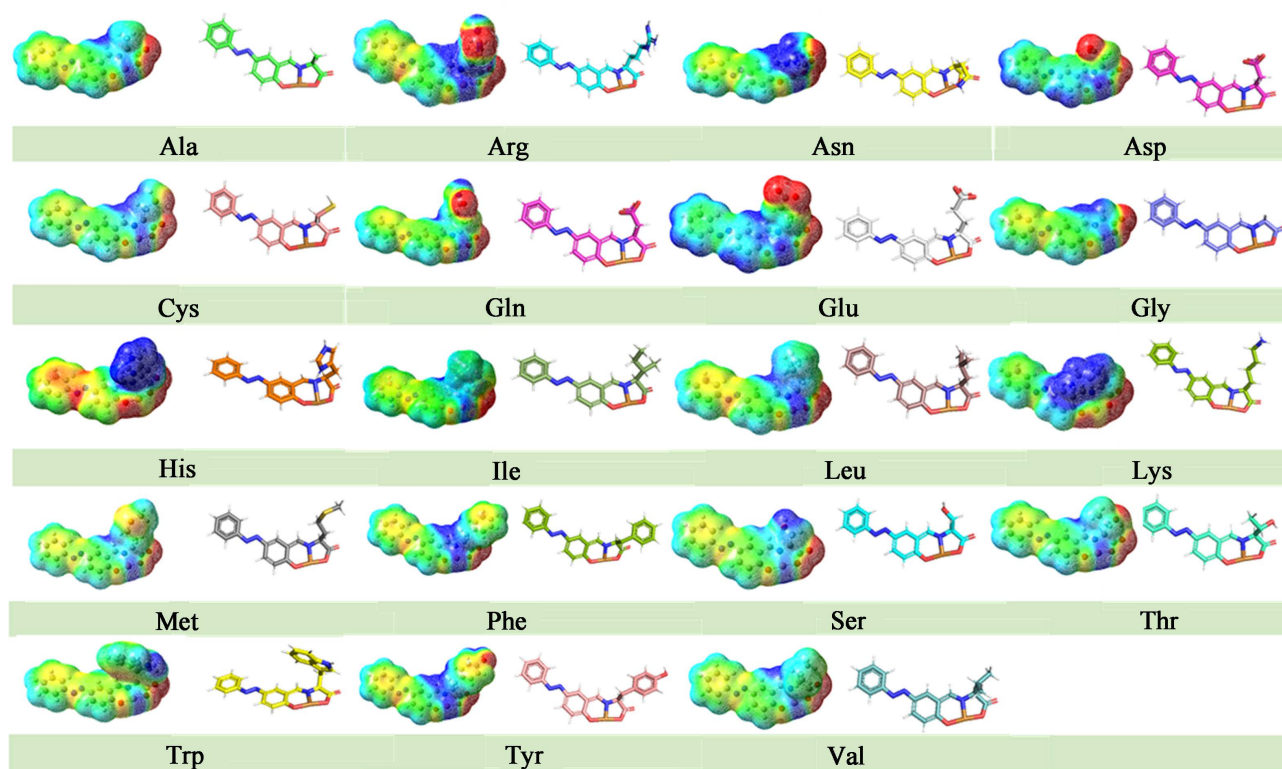


Figure 6. Electrostatic potential maps of 19 azobenzene-amino acid Schiff base copper(II) complexes as optimized structure based on DFT calculations.

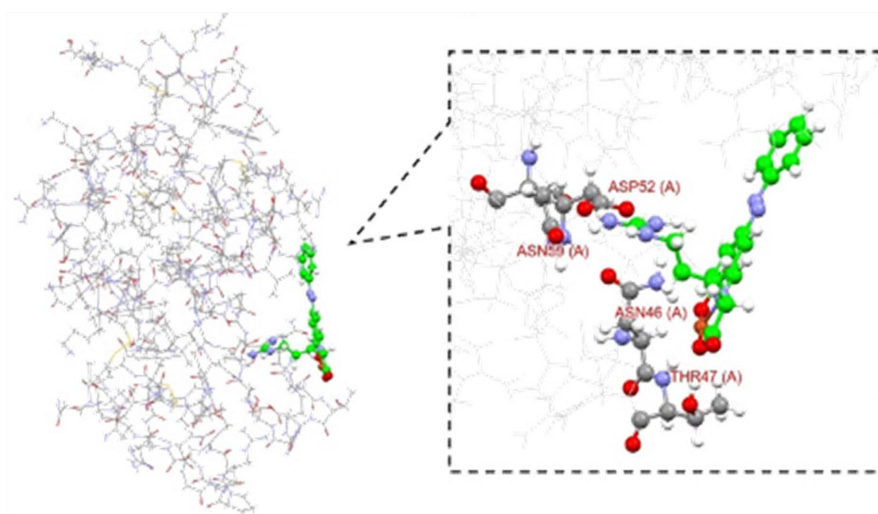


Figure 7. Docking simulation of CuAA@Lysozyme.

On the other hand, CuAT showed the highest Gold score (40.0124) in the manner in which the complex site other than the azo group docks in the hydrophobic pocket of lysozyme (**Figure 8**). The nearby amino acid residues of lysozyme include GLU (35)/ASN (46)/ASP (52)/ALA (110), which are 2.176 Å, 2.636 Å, 1.482 Å and 2.665 Å from the complex, respectively. It was a distance of GLU (35) and ALA (110) are positioned close to the copper site of the complex. ASN (46)

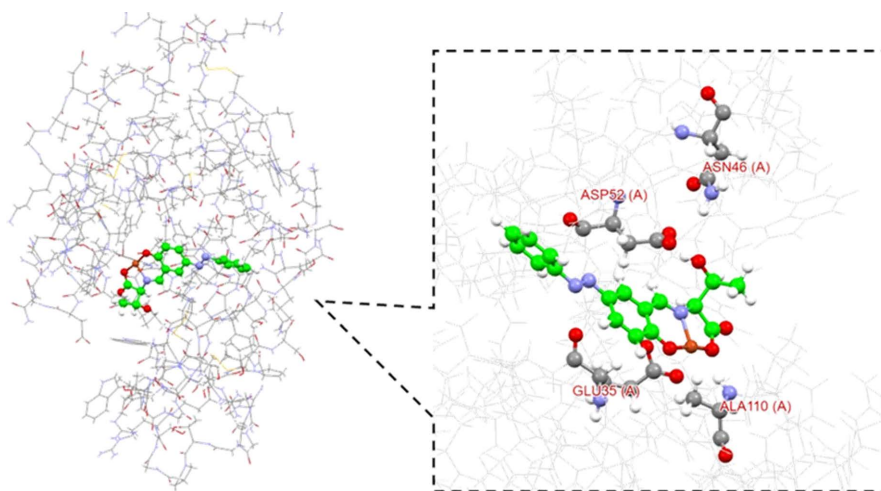


Figure 8. Docking simulation of CuAT@Lysozyme.

is in close proximity through a hydrogen bond with the -OH oxygen of Thr, and ASP (52) is in close proximity through a hydrogen bond with the -OH hydrogen. The complex has a hydrophobic pocket with copper facing the lysozyme and the azo moiety exposed to the outside.

Looking at the results, it can be seen that there are complexes that enter around the large dent in lysozyme and complexes that are docked to the entire lysozyme. The reason for this is thought to be that the introduction of an azo group into the conventional complex increased the bulkiness of the entire complex.

In this study, when synthesizing 19 kinds of amino acids based on the Gold score as ligands, lysozyme has certain solubility in either phosphate buffer, acetate buffer, or HEPES, which maintains the secondary structure of lysozyme, Thru, and Arg were used as ligands. Regarding Thr, as we have already introduced in previous research, in the copper(II) complex to be molecularly designed this time, the complex with lysozyme was confirmed by protein crystal structure analysis in the copper(II) complex without an azobenzene moiety. We also compare the interaction with lysozyme by protein crystallography under certain conditions. In addition, we will analyze the synthesis of Arg, which is one of the polar charged amino acids.

5. Conclusion

After confirming the conjugation by fluorescence quenching, lysozyme amino acid residues showed fluorescence at 300 - 400 nm at an excitation wavelength of 280 nm, indicating that a copper(II) complex existed in the vicinity of these sites. The shift of the fluorescence maximum wavelength to a longer wavelength is due to deprotonation of protons in the -NH- in the five-membered ring of Trp or in the -OH group at the end of Tyr. However, since pH 7.0 phosphate buffer was used in this experiment, it is reasonable to consider that the proton of -OH group in Tyr was deprotonated in this case. This agrees with the results from the

GOLD simulation. In CV, the current value decreased overall when lysozyme was added to the copper(II) complex. We also think that the bulkiness of lysozyme inhibited the transfer of electrons between copper(II) and the electrode. From the ESR spectra, it was suggested that the coordination environment of the copper(II) complex changed to planar or square pyramidal from the change in g value and spectral shape before and after lysozyme conjugation. UV-vis measurement confirmed the photoisomerization of the copper(II) complex even under the complex solution. The binding mode was considered by computational chemistry, though not preliminarily but completely crystallographic verification (binding features by using protein crystallography (**Figure 9**) as well as coordination geometry of copper(II) complexes by using powder crystal structure analysis) will be presented elsewhere soon.

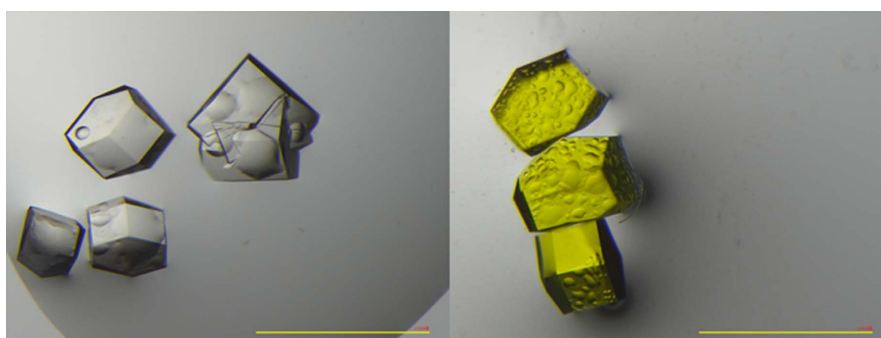


Figure 9. Single crystals of lysozyme (left) and CuAA@Lysozyme (right). According to preliminary results, CuAA's and CuAT's coordination bonding residue of lysozyme were confirmed identical to computational simulation.

Acknowledgements

This work was partially supported by a Grant-in-Aid for Scientific Research (A) KAKENHI (20H00336). The authors thank Prof. Masaki Unno (Ibaragi University) and Dr. Kenichi Kitanishi (Tokyo University of Science) for preliminary experiments in protein crystallography. The computation was performed using Research Center for Computational Science, Okazaki, Japan (Project: 22-IMS-C). This study was partly supported by the University of Tokyo Advanced Characterization Nanotechnology Platform in the Nanotechnology Platform Project sponsored by the Ministry of Education, Culture, Sports, Science and Technology (MEXT), Japan (JPMXP09-A-22UT0420).

Conflicts of Interest

The authors declare no conflicts of interest regarding the publication of this paper.

References

- [1] Andreini, C., Bertini, I., Cavallaro, G.L. and Thornton, J.M. (2008) Metal Ions in Biological Catalysis: From Enzyme Databases to General Principles. *Journal of Biological Inorganic Chemistry*, **13**, 1205-1218.
<https://doi.org/10.1007/s00775-008-0404-5>

- [2] Stappen, C.V., Deng, Y., Liu, Y., Heidari, H., Wang, J.-X., Zhou, Y., Ledray, A.P. and Lu, Y. (2022) Designing Artificial Metalloenzymes by Tuning of the Environment beyond the Primary Coordination Sphere. *Chemical Reviews*, **122**, 11974-12045. <https://doi.org/10.1021/acs.chemrev.2c00106>
- [3] Dabis, H.J. and Ward, T.R. (2019) Artificial Metalloenzymes: Challenges and Opportunities. *ACS Central Science*, **5**, 1120-1136. <https://doi.org/10.1021/acscentsci.9b00397>
- [4] Gandin, V., Porchia, M., Tisato, F., Zanella, A., Severin, E., Dolmella, A. and Marzano, C (2013) Novel Mixed-Ligand Copper(I) Complexes: Role of Diimine Ligands on Cytotoxicity and Genotoxicity. *Journal of Medicinal Chemistry*, **56**, 7416-7430. <https://doi.org/10.1021/jm400965m>
- [5] Nishihara, H. (2005) Combination of Redox- and Photochemistry of Azo-Conjugated Metal Complexes. *Coordination Chemistry Reviews*, **249**, 1468-1475. <https://doi.org/10.1016/j.ccr.2004.11.009>
- [6] Kashiwagi, K., Tassinari, F., Haraguchi, T., Banerjee-Gosh, K., Akitsu, T. and Naaman, R. (2020) Electron Transfer via Helical Oligopeptide to Laccase Including Chiral Schiff Base Copper Mediators. *Symmetry*, **12**, Article 808. <https://doi.org/10.3390/sym12050808>